COMMUNICATIONS CHEMISTRY

ARTICLE

https://doi.org/10.1038/s42004-019-0116-5 OPEN

Aerobic oxidative cleavage of 1,2-diols catalyzed by atomic-scale cobalt-based heterogeneous catalyst

Huihui Luo[1,2], Lianyue Wang[1], Sensen Shang[1], Jingyang Niu[2] & Shuang Gao[1]

The oxidative cleavage of the C–C bonds in 1,2-diols is an important transformation in synthetic organic chemistry. The challenge for this reaction is to develop a recyclable catalyst and an efficient catalytic system that operates under mild conditions. Here we report an atomically dispersed cobalt (3.8 wt% Co) on N-doped carbon catalyst, which exhibits improved catalytic activity toward the oxidative cleavage of a variety of 1,2-diols into esters, ketones or aldehydes using molecular oxygen under mild conditions. For example, the oxidative cleavage of internal diols is achieved at ambient temperature and air pressure. The robust catalyst can be reused at least seven times without regeneration treatment. The formation of highly dispersed active Co-N_x sites is demonstrated by catalyst characterization and potassium thiocyanate poisoning experiment. Mechanistic insights into monosubstituted diols indicate a sequence reaction including stepwise oxidation/nucleophilic addition/C–C bond cleavage, and reveal two reaction pathways.

[1] Dalian National Laboratory for Clean Energy, Dalian Institute of Chemical Physics, Chinese Academy of Sciences, 116023 Dalian, China. [2] Henan Key Laboratory of Polyoxometalate Chemistry, Institute of Molecular and Crystal Engineering, College of Chemistry and Chemical Engineering, Henan University, 475004 Kaifeng, China. Correspondence and requests for materials should be addressed to L.W. (email: lianyuewang@dicp.ac.cn) or to S.G. (email: sgao@dicp.ac.cn)

The oxidative cleavage of the C–C bonds in 1,2-diols to the corresponding carbonyl compounds is one of the most important transformation in synthetic organic chemistry[1]. The Malaprade reaction and the Criegee oxidation are classical methods for cleaving the C–C bond of 1,2-diols, which use stoichiometric or excess amount oxidants, such as periodic acid and its salts or lead tetraacetate (Fig. 1a)[2,3]. Up to now, these two methods remain the most widely used for vicinal diols cleavage. Other oxidants, such as chromium trioxide, manganese dioxide, and pyridinium chlorochromate have also been studied[4]. But these oxidants produce equimolar quantities of toxic waste and cannot meet the current environmental sustainable development needs. Therefore, the development of catalytic oxidation processes with a clean oxidant such as molecular oxygen is an alternative and promising protocol. A number of homogeneous transition-metal catalytic systems have been studied in the early time (Fig. 1b)[5–13]. Although these catalytic systems are capable of cleaving simple diols with molecular oxygen, most of them are still suffering from drawbacks such as low product selectivity, limited substrate range, the use of expensive noble metals (e.g., Pd, Ru), the required harsh conditions, activating sacrificial substrates, and no reusability of the catalyst. Very recently, Giulia Licini and co-workers reported vanadium-catalyzed aerobic C–C bond oxidative cleavage of vicinal diols under relatively mild conditions (80–100 °C) in different solvents, with a large variety of diols, affording the corresponding carbonyl derivatives[14]. Another recent example of mild silver(I)-catalyzed oxidative cleavage of 1,2-diols into carboxylic acids with wide adaptability was reported by Li and co-workers[15]. However, a critical drawback persists as these catalysts are homogeneous and suffer from the pervasive difficulty in recovery and reuse. Heterogeneous catalysis can address this limitation, but heterogeneous catalysts usually have the disadvantage of low activity. Some noble metal heterogeneous catalysts (such as Pt, Ru, and Au) were used for the oxidative cleavage of 1,2-diols[16–18]. Only one example was reported by Escande and co-workers for the oxidative cleavage of 1,2-diols using a heterogeneous catalyst based on non-noble metal manganese and sodium at 100 °C with a limited substrate rang (Fig. 1c)[19,20]. Hence, the development of sustainable and cost-efficient heterogeneous catalysts for the selective aerobic oxidative cleavage of 1,2-diolsunder mild reaction conditions still remains one of the most challenging issues.

Our recent investigations on the use of noble-metal-free nanoparticles deposited on nitrogen-doped carbon materials for various organic transformations led us to study the application of a promising heterogeneous catalyst for the oxidative cleavage of 1,2-diols[21–24].

Herein, we report an atomically dispersed Co-based heterogeneous catalyst supported on nitrogen-doped carbon materials with improved catalytic performance in the aerobic oxidative cleavage of a variety of 1,2-diols into esters, aldehydes or ketones under mild conditions with O_2 or air as the oxidant. The ability to cleave a variety of internal 1,2-diols at room temperature or 50 °C is a significant advantage compared to the previous reports (reaction temperature up to 100 °C)[19,20]. The robust catalyst can be recycled several times without loss of activity. The cobalt catalyst with well-dispersed Co–N_x sites on mesoporous N-doped carbon is synthesized by pyrolysis of well-defined natural vitamin B_{12} via hard template method. The studies of catalyst characterization and control experiments improve our understanding of the active species and the reaction process.

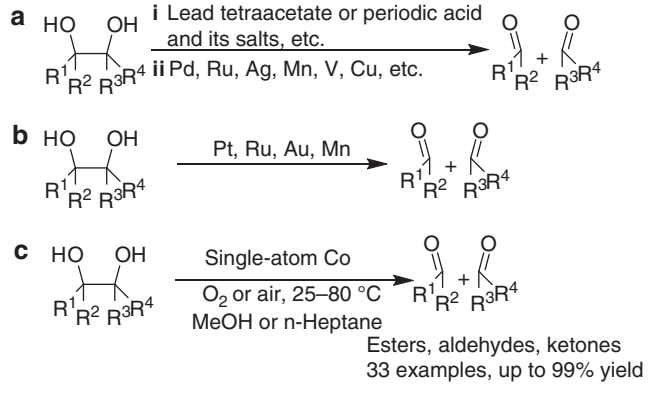

Fig. 1 Synthesis routes for previous and this work. **a** The first reaction with (classical methods) and (homogeneous transition metals) labeled as (**i**) and (**ii**). **b** Heterogeneous catalysis. **c** This work: heterogeneous non-noble metal catalyst with excellent reusability, mild reaction conditions, broad substrate range and mechanistic Insight

Results

Catalyst preparation. Supplementary Fig. 1 shows the simple preparation process for the cobalt catalyst according to our previous report with slight modification. The as-obtained catalysts are labeled as meso-Co-NC-*X* (meso: mesoporous; *X*: pyrolysis temperature).

Screening catalysts and optimizing the reaction conditions. Initially, the oxidative cleavage of 1-phenylethane-1,2-diol (**1a**) in MeOH to produce methyl benzoate (**2a**) was used as a model reaction to evaluate the abilities of the catalysts (Fig. 2). Firstly, the results from blank experiments indicated that the reaction did not proceed only in the presence of K_2CO_3 (Table 1, entry 1), and that the catalyst precursors gave no product **2a** without the high temperature pyrolysis process (Table 1, entry 2). The pyrolysis temperature greatly affected the catalytic activity (Table 1, entries 3–7). Meso-Co-NC-800 showed the best catalytic performance to produce **2a** in 96% yield (Table 1, entry 5). To unveil the underlying factors affecting the catalytic activity, the pore textural properties of the meso-Co-NC-*X* were analyzed by N_2 adsorption/desorption. The surface areas, total pore volume and pore size of meso-Co-NC-*X* catalysts were shown in Supplementary Table 1. The results showed that the specific surface area was positively related to the catalytic efficiency of the prepared catalysts with different pyrolysis temperatures. Meso-Co-NC-800 with the highest specific surface area and total pore volume exhibited the best catalytic activity compared with the other four catalysts. Meso-Co-NC-600 showed a lower catalytic activity, which might not only be attribute to the lower specific surface area, but also the lower pore volume and the lower pore size. In order to prove the crucial role of the cobalt species surviving from the acid treatment in this reaction, the vitamin B_{12} analogue phthalocyanine is used as precursor to obtain the catalyst through the same preparation method. The resulting catalyst meso-Pc-800 has no activity in the reaction (Table 1, entry 8). No reactivity was observed under N_2 atmosphere or in the absence of K_2CO_3 (Table 1, entries 9 and 10) indicating that O_2 and K_2CO_3 were necessary to achieve this reaction. Other inorganic bases were also screened in Supplementary Table 2. K_2CO_3 was turned out to be the best additive. When template SiO_2 was not removed, only

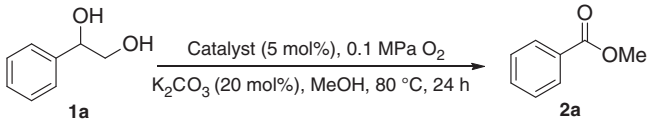

Fig. 2 Model system used for reaction optimization. Conditions used for optimization of the catalyst can be found in Table 1

Table 1 Oxidation of 1-phenylethane-1,2-diol promoted by different catalysts

Entry	Catalysts	Conv. (%)[a]	Yield (%)[b]
1	-	-	-
2	VB_{12}	24	-
3	meso-Co-NC-1000	75	72
4	meso-Co-NC-900	98	90
5	meso-Co-NC-800	100	96
6	meso-Co-NC-700	93	78
7	meso-Co-NC-600	71	43
8	meso-NC-800	-	-
9[c]	meso-Co-NC-800	-	-
10[d]	meso-Co-NC-800	-	-
11[e]	VB_{12}@SiO_2-800	39	15

Reaction conditions: 1-phenylethane-1,2-diol (0.25 mmol), K_2CO_3 (20 mol%), MeOH (4 mL), catalyst (5 mol%), 80 °C, 24 h
[a]Determined by LC analysis using biphenyl as internal standard
[b]Determined by GC analysis using biphenyl as internal standard and the product was confirmed by GC-MS
[c]0.1 MP N_2
[d]Without K_2CO_3
[e]Not washed with HF

15% of **2a** was obtained, suggesting the importance of mesoporous structure (Table 1, entry 11). Other reaction condition optimizations including catalyst loading, K_2CO_3 loading, air, and reaction temperature have been examined (Supplementary Table 2).

Stability study of catalyst. Encouraged by these promising results, we first need to confirm the heterogeneous nature of the catalyst. A leaching experiment was carried out by removing catalyst before the reaction was complete by simple hot-filtration test. The results showed that the yield of product did not increase further after the catalyst was filtered, suggesting that the catalytic process was truly heterogeneous (Supplementary Fig. 2). Then, the stability and recyclability of the meso-Co-NC-800 were examined. After reaction, the catalyst was filtrated off, washed with methanol and dried under vacuum. What is noteworthy is that the regeneration treatment of the used catalyst is not needed, when the next cycle is conducted. The catalyst was run for six consecutive times without any loss of activity (Supplementary Fig. 3).

Catalyst characterization. N_2 adsorption/desorption analysis showed the mesoporous structure of the as-obtained catalysts, and the Brunauer–Emmett–Teller (BET) surface area and the average pore size were 659.7 $m^2 g^{-1}$ and 12.5 nm, respectively (Supplementary Fig. 4). XRD diffractogram did not reveal anycobalt metal or its oxide peaks, indicating that the Co species in the sample are either highly dispersed or amorphous (Supplementary Fig. 5).The morphology of catalyst was characterized by electron microscopy techniques. SEM images under UED detector mode with 1.0 keV accelerating voltages showed honeycomb mesoporous structure of the meso-Co-NC-800 catalyst (Supplementary Fig. 6a, and more images see Supplementary Figure 7a–c). No cobalt-containing nanoparticles were detected on the surface of the meso-Co-NC-800, which is in good agreement with the XRD results. The result was confirmed under BED-C mode 15 keV accelerating voltages (Supplementary Fig. 6b, and more images see Supplementary Figure 7d, e, f). The same conclusion was reached from HRTEM and STEM images (Supplementary Fig. 6c-d, and more images see Supplementary Figure 8a–d). Nevertheless, from the STEM images, C, N, O, and Co elements were clearly observed on the surface of catalyst by energy-dispersive X-ray EDX analysis (Supplementary Fig. 9), and the corresponding element maps showed that these elements are evenly distributed throughout the structure (Supplementary Fig. 6e). Moreover, inductively coupled plasma atomic emission spectrometry (ICP-AES) and X-ray photoelectron spectroscopy (XPS) revealed approximately 3.8 wt% and 0.79 at% (corresponding to a weight percentage of 3.7 wt%) of cobalt survived the acid treatment, respectively. These results indicated that the cobalt species must be highly dispersed as subnanoscale level or single atoms that cannot be detected or visible by XRD, SEM, HRTEM, and STEM techniques. In order to obtain some information about the chemical state of cobalt at the atomic level, high angle annular dark field (HADDF) technique was per formed on an aberration-corrected JEM-ARM 200F microscope to observe the meso-Co-NC-800 catalyst (Supplementary Fig. 6f). It was observed that Co single atoms were uniformly dispersed on N-doped carbon materials. No agglomerated metallic cobalt or cobalt oxide are found in the whole detected region. Our previous investigation using Extended X-ray absorption fine-structure (EXAFS) indicated that at the Co K edge, the spectrum of meso-Co-NC-800 catalyst was different from the reference samples, Co foil, CoO, or Co_3O_4, further confirming that there exists no metallic cobalt or cobalt oxide particles in our catalyst[22].

To gain more information on the elemental compositions and chemical states of as-obtained catalysts, X-ray photoelectron spectroscopy (XPS) analysis was conducted. The survey of meso-Co-NC-X ($X = 600–1000$ °C) catalysts was shown in Supplementary Fig. 10. C, N, O, and Co elements were detected, which is consistent with EDX results. The content of each element in a series of meso-Co-NC-X catalysts was summarized in Supplementary Table 3. The content of Co, N decreases with the pyrolysis temperature increasing, while the content of C tends to increase. The general trend of oxygen content is reduced. Especially, when the temperature reaches 800 °C, the content of O is minimum. The XPS detailed analysis of the best active catalyst (meso-Co-NC-800) was given as following. The C1s spectrum reveals four types of carbon species: C=C at 284.6 eV, C=N at 285.7 eV, C−N 286.6 eV, and O−C=O at 289.2 eV, which indicates N atoms successfully doped in the VB_{12} derived materials (Supplementary Fig. 11a)[25]. The high-resolution O1s spectrum shows the existence of carbon atoms bonded with oxygen atoms (Supplementary Fig. 11b). The high-resolution N1s spectrum was fitted into four peaks: pyridinic or N–Co (398.5 eV), pyrrolic (400.2 eV), graphitic (401.0 eV), and oxidized nitrogen (403.9 eV) (Supplementary Fig.11c)[26,27]. The proportion of pyridine nitrogen is greatest (accounting for 47.9% in total N species). It is important to note that the peak value of 398.6 eV should also include N–Co contribution, because the N–Co has a binding energy close to the pyridinic N. The Co XPS spectrum showed two main peaks at 780.9 eV and 795.9 eV, which are attributed to Co $2p_{3/2}$ and Co $2p_{1/2}$, respectively (Supplementary Fig. 11d). The low energy bands can be deconvoluted into two peaks: Co–O (780.0 eV), Co–N (781.7 eV)[28,29]. This type of Co–N was well in agreement with the N–Co species detected from N1s spectrum. These results demonstrated the existence of the coordination of Co species with N atoms in the graphitic layer ($Co–N_x$). This coordination environment not only resists against either aggregation during the subsequent heat treatment or leaching by acid treatment, but also plays a key role in improving the activity of catalyst[30–32].

XPS measurements were also used to analyze the effect of pyrolysis temperature on the possible bonding between Co and N or O in catalysts. As shown in Supplementary Table 3, 800 °C affords the highest ratio of Co/N, which indicated that the density of $Co–N_x$ active sites is the largest. In addition to Co–N, the peak Co–O was also detected in Co XPS spectrum. The cobalt

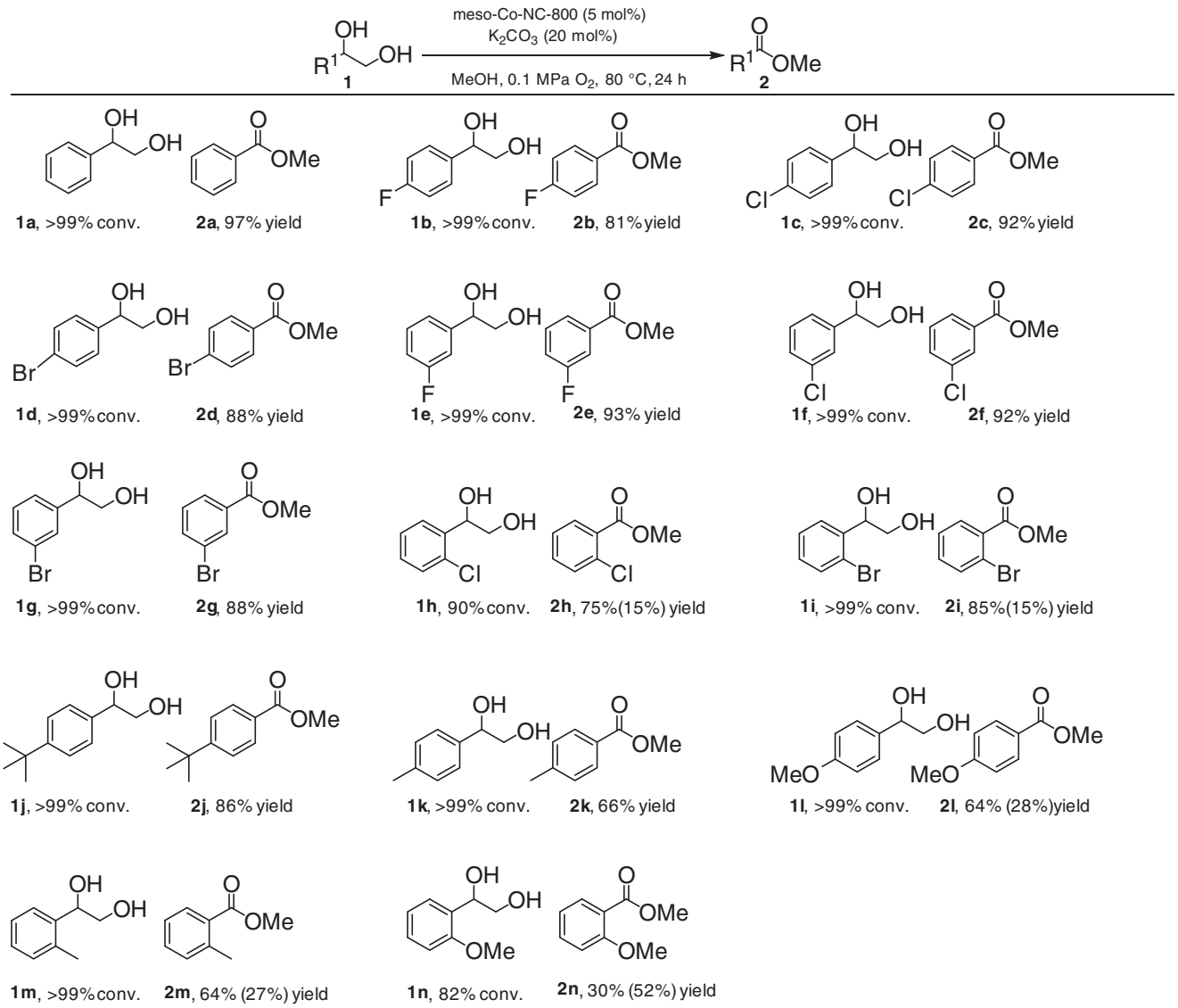

Fig. 3 Aerobic oxidative cleavage of monosubstituted 1,2-diols to esters. Reaction conditions: 1,2-diol (0.25 mmol), MeOH (4 mL). Conversion was determined by HPLC using biphenyl as internal standard. Yield was determined by GC using biphenyl as internal standard and the product was confirmed by GC-MS, values in parentheses correspond to yield of aldehydes

coordination environment may also involve oxygen atoms[33]. Excessive oxygen atoms saturate the cobalt and may reduce the cobalt active sites. It should be noted that the ratio of Co/O at 800 °C is much higher than other pyrolysis temperature, indicating the existence of much more Co unsaturated sites. These results suggest that nitrogen-coordinated maximum atomic Co sites produced the largest density of Co–N_x active sites with the best activity.

Catalyst poisoning experiment. To further shed light on this viewpoint that Co–N_x species was the primary active sites in the target reactions, the poisoning experiment was performed with KSCN as binding molecule, which would interrupt the metal-centered active site and inhibit the catalyst toward the reaction. Amount of KSCN was mixed with catalyst in MeOH at 60 °C for 1 h, and then the reaction was conducted under standard conditions. The results indicated that the catalytic activity was significantly reduced (Supplementary Fig. 12).

Scope of the present reaction. With the optimal conditions in hand, we applied the catalytic method to other substrates (Fig. 3). The electron-deficient mono-substituted aromatic 1,2-diols (**1a**–**1i**) afforded the desirable products (**2a**–**2i**) in good to excellent yields. The electron-rich mono-substituted aromatic1,2-diols (**1j**–**1n**) gave the desirable products (**2j**–**2n**) in moderate to good yields. The corresponding major by-products were aldehydes. It seems that the position of the substitutes on the benzene ring has no obvious effect on cleavage of C–C bond under the optimized conditions. But the electron properties of substituents have a greater effect on the chemoselectivity of the reaction.

To further expand the substrate scope of this catalytic system, internal diols were also tested in this catalytic system. Firstly, we use (*S*,*S*)-hydrobenzoin (**3a**) to optimize the reaction temperature (Supplementary Table 4). It was found that the heterogeneous catalytic system can realize the oxidative cleavage of this kind of substrates at room temperature. The results are summarized in Fig. 4. Both meso- and (*S*,*S*) or (*RR*)-hydrobenzoin (**3a**–**3c**) were cleaved efficiently. When air replaces pure oxygen as the oxidant, the yield of 91% is still available. The substrates (**3d**–**3e**) containing an electron-withdrawing group at the aryl ring could be transformed to the desired products (**2b**, **2d**) in excellent yields. However, **3f** employed as substrate led to a low yield, and

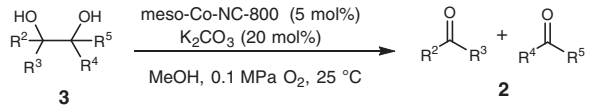

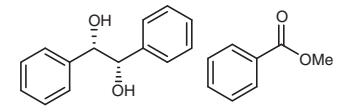
3a, >99% conv. **2a**, 95% yield

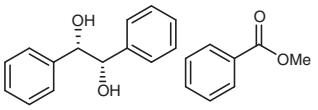
3a, >99% conv. **2a**, 91% yield[a]

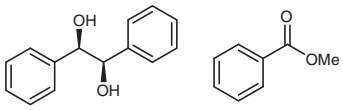
3b, >99% conv. **2a**, 98% yield

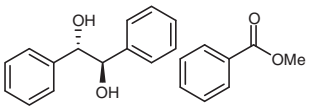
3c, >99% conv. **2a**, 99% yield

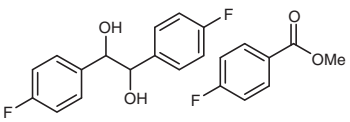
3d, >99% conv. **2b**, 93% yield

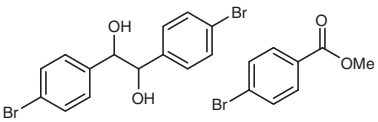
3e, >99% conv. **2d**, 95% yield

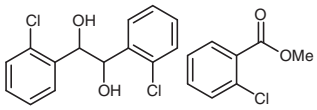
3f, >99% conv. **2h**, 38% (64%)/ 84% (12%) yield[b]

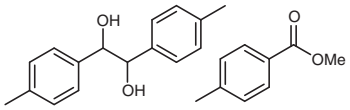
3g, >99% conv. **2k**, 70% (21%) yield

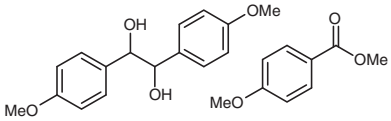
3h, >99% conv. **2l**, 68% (9%) yield

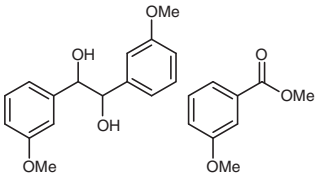
3i, >99% conv. **2o**, 97% yield

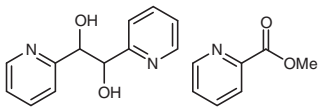
3j, >99% conv. **2p**, 99% yield

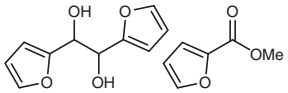
3k, >99% conv. **2q**, 5% (61%) yield

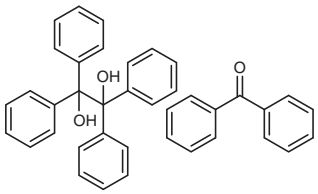
3l, >99% conv. **2r**, 92% yield

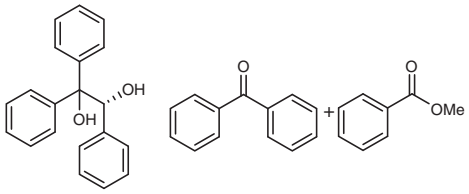
3m, >99% conv. **2r**+**2a**, 100%+76% (24%) yield

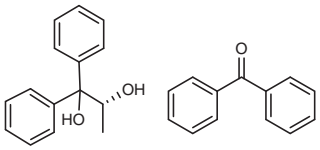
3n, >99% conv. **2r**, 95% yield[c]

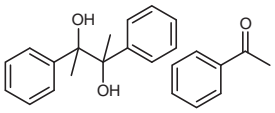
3o, >99% conv. **2s**, 96% yield[c]

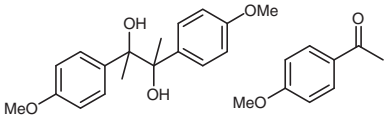
3p, >99% conv. **2t**, 94% yield[c]

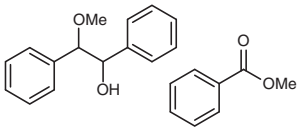
3q, >99% conv. **2a**, 91% yield[b]

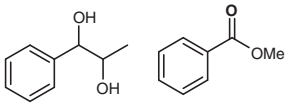
3r, >99% conv. **2a**, 83% yield

Fig. 4 Aerobic oxidative cleavage of internal 1,2-diols. Reaction conditions: 1,2-diol (0.25 mmol), K_2CO_3 (20 mol%), meso-Co-NC-800 (5 mol%), MeOH (4 mL), 0.1 MPa O_2, 25 °C, **3a** 14 h, **3b**–**3r** 24 h. Conversion was determined by HPLC using biphenyl as internal standard. Yield was determined by GC using biphenyl as internal standard and the product was confirmed by GC-MS, values in parentheses correspond to yield of aldehydes. [a]Air as the oxidant, [b]80 °C, [c]50 °C

afforded 2-chlorobenzaldehyde in 64% yield. Substrates (**3g**–**3i**) with electron-rich aryl substituents gave the corresponding products (**2k**–**2o**) in good to excellent yield. The major products were the corresponding aldehydes, which might be due to the low reaction temperature (25 °C). The aldehyde is not easily converted to the corresponding ester at 25 °C. When the temperature was increased to 80 °C, **2h** could be obtained in 84% yield with only 12% yield of o-chlorobenzaldehyde. The cleavage of heteroaryl 1,2-diol (**3j**) containing pyridine fragment, proceeded smoothly to generate heterocyclic esters **2p** in 99%

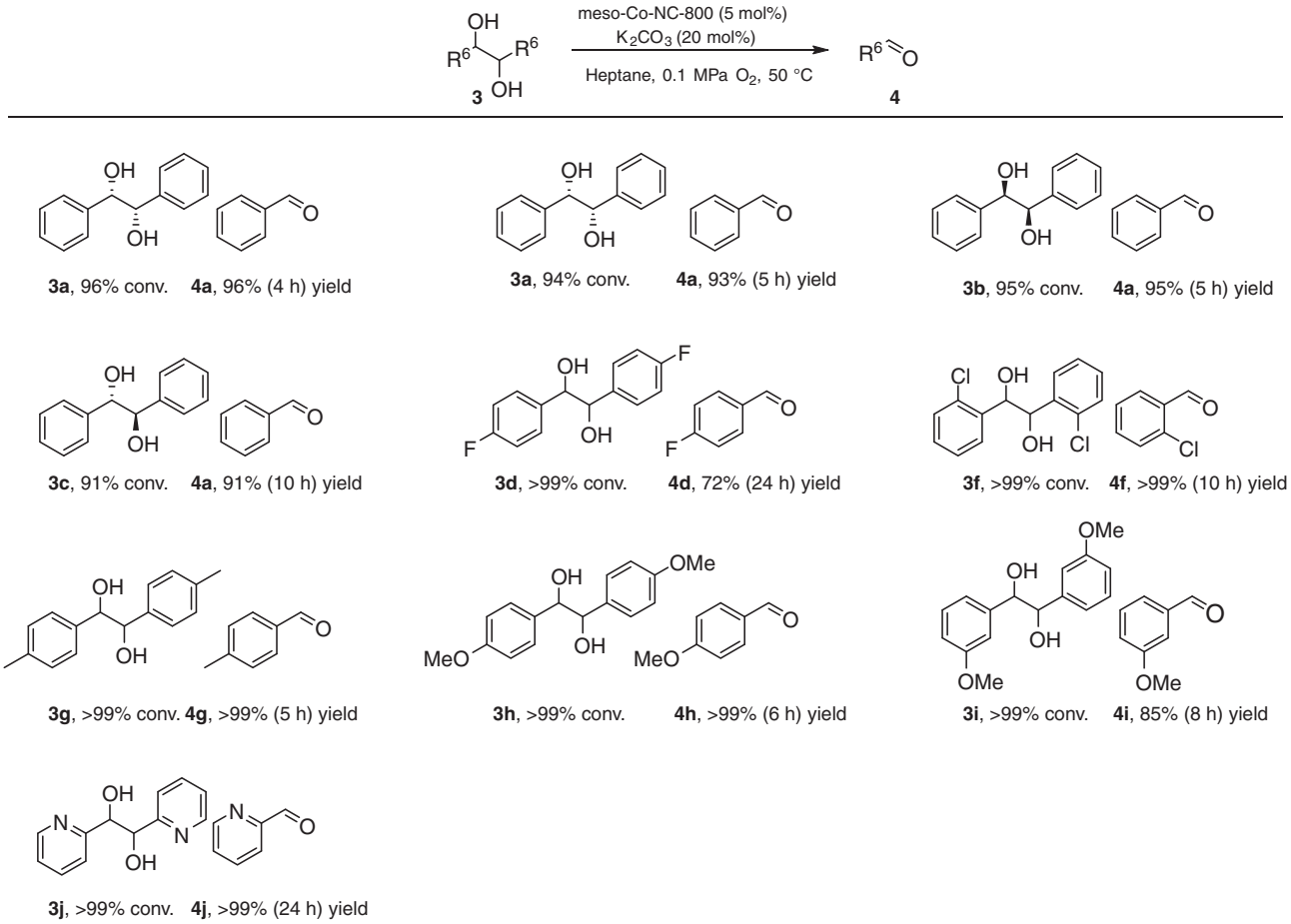

Fig. 5 Aerobic oxidative cleavage of internal 1,2-diols to aldehydes. Reaction conditions: 1,2-diol (0.25 mmol), n-Heptane (4 mL), 4–24 h. Conversion was determined by HPLC using biphenyl as internal standard. Yield was determined by GC using biphenyl as internal standard and the product was confirmed by GC-MS. [a]Air as the oxidant, [b]80 °C

yield. But Furan 1,2-diol (**3k**) gave 61% yield of aldehyde. Several benzopinacol substrates (**3l**–**3p**) were subjected to the variable reaction conditions. The corresponding ketones (**2r**–**2t**) were obtained in excellent yield. One of the hydroxyl groups is protected by the methyl group (**3q**), giving **2a** in 91% yield by raising the reaction temperature. It is noteworthy that the catalytic system is also effective for less activated internal diols (**3r**).

To further extend the range of application, this catalytic system was used to cleave C–C bonds of internal 1,2-diols to produce aldehydes, which could be used for further transformations (Fig. 5). The reaction conditions were optimized with (*S*,*S*)-hydrobenzoin (**3a**) as the model substrate (Supplementary Table 5). A variety of 1,2-diols with electron-donating and with drawing aromatic substituents, afforded the corresponding products in good to excellent yields (**3a**–**3d**, **3f**–**3j**). Notably, the substrate **3f** bearing o-chloro substituents underwent quantitative cleavage into the corresponding aldehyde **4f** in quantitative yield. The catalytic system can also effectively oxidize the diols containing heteroatoms into the corresponding aldehyde (**3j**).

The synthetic utility of the present catalyst is further evaluated in multistep, one-pot reaction sequences. A variety of transformations of 1,2-diols are achieved in Fig. 6. All the desired products were obtained in good to excellent yields, suggesting that the catalyst is of high efficiency and multiple catalytic capacities.

The gram-scale experiment was performed using 1-phenylethane-1,2-diol as a test substrate. The target product was obtained in 85% yield even with the catalyst loading reduced to 2.5 mol%. The result indicates that the heterogeneous Co-based catalytic system shows high activity, selectivity, and practicability for the aerobic oxidative cleavage of 1,2-diols under mild reaction conditions.

Mechanistic studies. To gain more insights into the mechanism of this transformation, several control experiments were carried out. First, a radical scavenger e.g., 2,2,6,6-tetramethyl-1-piperidinyloxy (TEMPO), 2,6-di-tert-butyl-4-methylphenol (BHT), or acrylamide is used to determine whether the reaction is a free radical process. When TEMPO, BHT, or acrylamide was added into the reaction mixture, the target product was obtained in 87%, 85%, and 80% yields, respectively, thus suggesting that this reaction might not involve free radicals.

Next, some compounds derived from 1,2-diols as potential intermediates were examined in the reaction system (Fig. 7a). In addition to benzoic acid, all possible derivatives gave excellent yield under standard reaction conditions, while different reaction results were given in terms of shortening the reaction time. It was found that when 2-hydroxy-1-phenylethanone (**5a**), phenylglyoxal monohydrate (**5c**), mandelic acid (**5d**), and benzoylformic acid (**5e**) were employed as the substrates, the reaction was much faster for the latter than for the former. These results suggest a stepwise oxidation of α-hydroxy group through the oxidation of **5a** (or the tautomer **5b** as well, which is a tautomer of **5a**) to **5c** (**5d**), and further to **5e**.

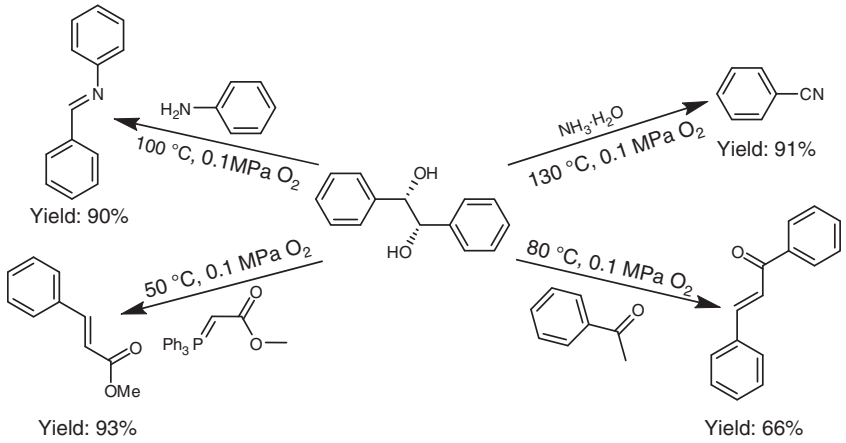

Fig. 6 Application of meso-Co-NC-800-catalyzed aerobic oxidative cleavage of 1,2-diols in tandem reactions. Reaction conditions: substrates (0.25 mmol), meso-Co-NC-800 (5 mol%), K_2CO_3 (20 mol%), n-Heptane (4 mL), 24 h. No K_2CO_3 is required for the synthesis of benzonitrile

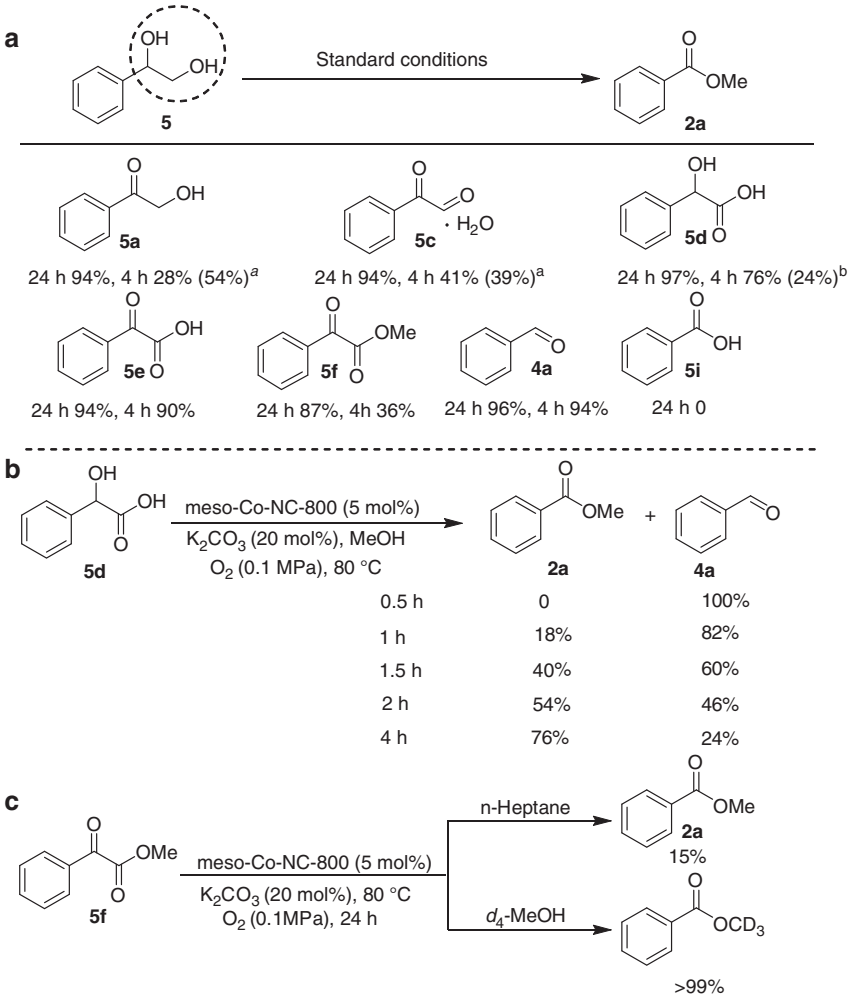

Fig. 7 Control experiments. **a** Some compounds derived from 1,2-diols as potential intermediates were examined in the reaction system. **b** Reaction evolution of mandelic acid with different reaction times. **c** The necessity of alcohol. [a]The value in parentheses is the yield of methyl benzoylformate (**5f**). [b]The value in parentheses is the yield of benzaldehyde (**4a**)

When possible intermediates **5a** and **5c** were subjected to the standard conditions, ketoester (**5f**) was also obtained in 54% and 39% yield, respectively, and the yield of the **5f** decreased gradually, thus implying that the formation of **5f** was from the reaction of nucleophilic addition of the aldehyde group of **5c** with MeOH. It's worth noting that the reaction of **5a**, **5c**, **5e**, and **5f** under the standard conditions did not give aldehyde (**4a**).

When possible intermediate **5d** was subjected to the standard conditions, **4a** was obtained in 24% yield within 4 h. The result promoted us to investigate the reaction evolution of **5d** with

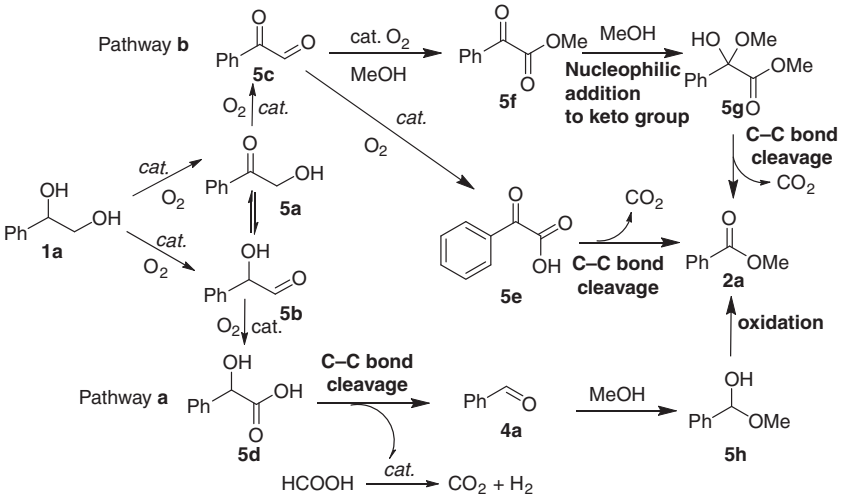

Fig. 8 Possible reaction mechanism for the cleavage of monosubstituted diols. Pathway **a** the oxidative cleavage of 1-phenylethane-1,2-diol **1a** underwent the intermediate benzaldehyde **4a**. Pathway **b** the oxidative cleavage of 1-phenylethane-1,2-diol **1a** underwent the intermediates ketoester **5f** and benzoylformic acid **5e**

different reaction times (Fig. 7b). It was found that the quantitative aldehyde was obtained in 0.5 h. No **2a**, **5e**, and **5f** were detected. These results demonstrated that **4a** was from **5d**. The yield of **2a** increased with the extension of the reaction time, while the yield of **4a** decreased gradually. These results suggested that the nucleophilic addition of **4a** with MeOH formed the hemiacetal and that the hemiacetal was subsequently oxidized to the ester (**2a**). In addition, formic acid was obtained along with the C–C bond cleavage of **5d**, and then the formic acid decomposed to CO_2[34], which was detected by the lime-water-test (Supplementary Fig. 13). When possible intermediate **5e** was subjected to the standard conditions, **2a** was obtained in 90% yield within 4 h. Such a fast reaction rate leads to a further reduction reaction time, with 56% yield of **2a** being achieved in just 0.5 h. These results demonstrated that compound **5e** rapidly cleave C–C bonds without passing through intermediate **5f** and that **5f** was not from **5e** but from **5c**, which was different from the previous work[35].

Then, the transformation of **5f** to **2a** was verified in Fig. 7c. Only 15 % of **2a** was detected when the reaction was performed in n-heptane instead of MeOH. In order to further prove the necessity of alcohol, **5f** was subjected to the standard conditions in d_4-MeOH. The desired deuterated methyl benzoate was obtained in >99% yield. These results gave us a conclusion that the nucleophilic addition of the keto with MeOH took place in the conversion of **5f** to **2a**. The **2a** was obtained along with the C–C bond cleavage of **5f**. The methyl formate was hydrolyzed to MeOH and HCOOH. The resultant HCOOH was decomposed to CO_2 and H_2[34].

A kinetic study with time-dependent experiments on the oxidative cleavage of **1a** revealed the presence of benzaldehyde (**4a**) and ketoester (**5f**) (Supplementary Fig. 14a). The kinetic data did not fit well with the first-order rate equation with respect to diol, while followed the pseudo-second-order-rate equation very well with a rate constant of 0.219 mol L^{-1} h^{-1} (Supplementary Fig. 14b). The apparent activation energy of this reaction determined by an Arrhe-nius plot (60–80 °C) was 14.9 kJ mol^{-1} (Supplementary Fig. 15).

On the basis of the control experiment results and pertinent literature reports, a possible reaction mechanism was proposed (Fig. 8). Firstly, with the assistance of K_2CO_3, 1- phenylethane-1,2-diol (**1a**) was oxidized to the 2-hydroxy-1-phenylethanone (**5a**) (or the tautomer **5b** as well) by the active species generated from the activation of oxygen by the Co-based catalyst[36–40]. Then, there are two possible reaction pathways for this reaction. In pathway **a**, **5b** was oxidized to mandelic acid (**5d**) and then the C–C bond cleavage occurs to produce benzaldehyde (**4a**) with release of a CO_2. The addition of MeOH to **4a** afforded the hemiacetal intermediate **5h**. Subsequently, Co-catalyzed aerobic oxidation of the **5h** takes place, leading to the formation of ester **2a**. In pathway **b**, compound **5a** was oxidized to phenylglyoxal (**5c**). The addition of MeOH to **5c** formed the hemiacetal intermediate, and then hemiacetal intermediate underwent the oxidation to afford ketoester (**5f**) under standard conditions. The nucleophilic addition of the **5f** with MeOH gave the intermediate **5g**. Finally, the C–C bond cleavage of the **5g** produced the ester **2a**, along with the production of CO_2. And, in pathway **b**, there is another alternative. The compound **5c** is further oxidized to benzoylformic acid (**5e**), which rapidly cleaves the C–C bond to form the target product ester **2a** with this release of a CO_2.

To get more information about the reaction mechanism of the aerobic oxidative cleavage, isotope-labeling experiments were conducted with $^{18}O_2$ as the sole oxidant. Under our experimental conditions, $C^{18}O^{16}O$ ($m/z = 46$) was detected as by-products by mass spectrometry (Supplementary Fig. 16); Meanwhile, H_2 ($m/z = 2$) was also detected (Supplementary Fig. 17). The above results proved the oxygen transfer from O_2 to CO_2, further affirming the existence of the proposed reaction pathways.

In order to obtain more information on the mechanism of the cleavage of internal diols, time-dependent experiments on the oxidation of (*S*,*S*)-hydrobenzoin was conducted to study this reaction Kinetic (Supplementary Fig. 14c). At the initial reaction time, the aldehyde was obtained, but the target product ester was not detected. In addition, it has to be noted that benzil was not detected by GC-MS during the whole reaction process, and that when benzil was subjected to the standard reaction conditions, ester was obtained only in 18% yield. These results indicated that this reaction process refused to undergo benzil compound, which is different from some previous reports[15]. It was very interesting to find that trans isomer, meso-hydrobenzoin was fast cleaved faster than the cis isomer, (*S*,*S*)-hydrobenzoin (Supplementary Fig. 14d). The results indicated that this reaction process may be classified as a type II mechanism[41]. Free radical capture experiments have ruled out free radical process of the reaction (Supplementary Fig. 18). So we can speculate on such a conclusion that this type II mechanism involves the formation

of a monodentate complex between diol and active oxidant species, which then oxidatively collapses to the carbonyl product in a two-electron oxidation (Supplementary Fig. 19).

Discussion

In conclusion, we have developed a single-atom dispersed meso-Co-NC-based heterogeneous catalytic system for the aerobic oxidative C−C bond cleavage of 1,2-diols with O_2/air as the oxidants under mild reaction conditions. A series of diols could be efficiently cleaved and converted into the corresponding esters, ketones or aldehydes. Characterization results demonstrated that cobalt species are highly dispersed in the form of Co–N_x. The Co–N_x active site was further confirmed by the KSCN poisoning experiment. Mechanistic insights into the monosubstituted diol cleavage process reveal that two key intermediates introduce two different reaction pathways, and that a sequence reaction involves stepwise oxidation/nucleophilic addition/C–C bond cleavage. The reaction process of internal 1,2-diols followed a type II mechanism via two-electron oxidative fragmentation. Mild reaction conditions, non-noble metal catalyst, and excellent reusability of the catalyst make the present catalytic system much more competitive than the existing systems. This work also provides insights into the application of single atom catalyst (SAC) in C−C bond cleavage.

Methods

Synthesis and characterization. See Supplementary Methods for general information about chemicals, analytical methods and characterization for catalysts and substrates. NMR spectra are available in Supplementary Figures 20-42.

Preparation of meso-Co-NC-X catalyst. 2.5 g of LUDOX® AS-40 colloidal silica and 1.0 g VB_{12} were dissolved in 50 mL water for 30 min at room temperature under vigorous stirring. Then, the mixture was dried at 100 °C. The obtained VB_{12}@SiO_2 was grinded into powder and pyrolyzed in a flow of ultrapure nitrogen at 800 °C (or 600, 700, 900, and 1000 °C) for 2 h with the heating rate of 5 °C min^{-1}, then cooled naturally to room temperature. The samples were acid leached in HF (40 wt% hydrofluoric) for 24 h continuous agitation at room temperature to remove the silica template. Finally, the etched samples were thoroughly washed with de-ionized water until reaching a neutral pH and dried in vacuum at 100 °C overnight.

Procedures for the aerobic oxidative cleavage of monosubstituted 1,2-diols to esters. In a typical oxidation, 1-phenylethane-1,2-diol (0.25 mmol), meso-Co-NC-800 (5 mol%), K_2CO_3 (20 mol%) and MeOH (4 mL) were into a round-bottom flask (25 mL) with a magnetic bar. Then the resulting mixture was transferred to an autoclave. After the autoclave was closed, and purged with oxygen three times before it was finally pressurized for 24 h with an oxygen atmosphere, and stirred at 80 °C. After the reaction, the internal standard (biphenyl, 15 mg) and MeOH (1 mL) were added. The mixture analysis were performed on LC, GC and confirmed by GC-MS.

Procedures for the aerobic oxidative cleavage of internal 1,2-diols to esters. In a typical oxidation, (*S*,*S*)-hydrobenzoin (0.25 mmol) and meso-Co-NC-800 (5 mol%), K_2CO_3 (20 mol%) and MeOH (4 mL) were introduced into a round-bottom flask (25 mL) with a magnetic bar. Then the resulting mixture was transferred to an autoclave. After the autoclave was closed, and purged with oxygen three times before it was finally pressurized with an oxygen atmosphere. Subsequently, the tube was stirred at 25 °C for 24 h. After the reaction, the internal standard (biphenyl, 15 mg) and MeOH (1 mL) were added. The mixture were analyzed by LC, GC, and confirmed by GC-MS.

Procedures for the aerobic oxidative oxidation of internal 1,2-diols to aldehydes. In a typical oxidation, (*S*,*S*)-hydrobenzoin (0.25 mmol) and meso-Co-NC-800 (5 mol%), K_2CO_3 (20 mol%) and n-heptane (4 mL) were introduced into a round-bottom flask (25 mL) with a magnetic bar. Then the resulting mixture was transferred to an autoclave. After the autoclave was closed, and purged with oxygen three times before it was finally pressurized with an oxygen atmosphere. Subsequently, the flask was stirred at 50 °C. After the reaction, the internal standard (biphenyl, 15 mg) and n-heptane (1 mL) were added. The mixture were analyzed by LC, GC, and confirmed by GC-MS.

Large-scale and recycling test. 1-phenylethane-1,2-diol (7.5 mmol), meso-Co-NC-800 (2.5 mol%), K_2CO_3 (20 mol%) and MeOH (15 mL) were added into a round-bottom flask (50 mL) with a magnetic bar. Then the resulting mixture was transferred to an autoclave. After the autoclave was closed, and purged with oxygen three times before it was finally pressurized with an oxygen atmosphere. Subsequently, the flask was stirred at 80 °C for 48 h. After completion of the reaction, the liquid mixture was analyzed by LC, GC, and confirmed by GC-MS.

The catalyst was recovered by filtration, washing with MeOH and drying under vacuum to remove the residual solvent, and reused for the next run.

Data availability

All data that support the findings of this study are available within the paper and its Supplementary Information, or are available from the corresponding author upon reasonable request.

Received: 13 September 2018 Accepted: 8 January 2019
Published online: 14 February 2019

References

1. Perlin, A. S. in *Advances in Carbohydrate Chemistry and Bio-chemistry*, Vol. 60 (eds D. Horton) 183 (Academic Press, Cambridge, 2006).
2. Malaprade, L. Action of polyalcohols on periodic acid and alkaline periodates. *Bull. Soc. Chim.* **3**, 833–852 (1934).
3. Criegee, R. An oxidative fission of glycols (II. Communication. On oxidations with lead(IV)-salts)). *Ber. Dtsch. Chem. Ges.* **64**, 260–266 (1931).
4. Amadio, E., Lorenzo, R. D., Zonta, C. & Licini, G. Vanadium catalyzed aerobic carbon-carbon cleavage. *Coord. Chem. Rev.* **301-302**, 147–162 (2015).
5. Prati, L. & Rossi, M. Stepwise oxidation of 1,2-diols resulting from molecular oxygen activation by copper. *J. Mol. Catal.* **110**, 221–226 (1996).
6. Barroso, S. et al. Chemistry and reactivity of mononuclear manganese oxamate complexes: oxidative carbon–carbon bond cleavage of vic-diols by dioxygen and aldehydes catalyzed by a trans-dipyridine manganese(III) complex with a tetradentate o-phenylenedioxamate ligand. *J. Mol. Catal.* **243**, 214–220 (2006).
7. Riano, S., Fernandez, D. & Fadini, L. Oxidative cleavage of vic-diols catalyzed by manganese (III) complexes in ionic liquids. *Catal. Commun.* **9**, 1282–1285 (2008).
8. Takezawa, E., Sakaguchi, S. & Ishii, Y. Oxidative cleavage of vic-Diols to aldehydes with dioxygen catalyzed by $Ru(PPh_3)_3C_{l2}$ on active carbon. *Org. Lett.* **1**, 713–715 (1999).
9. Mastrorilli, P., Suranna, G. P., Nobile, C. F., Farinola, G. & Lopez, L. Aerobic oxidative cleavage of pinanediols by cobalt(II) acetylacetonate in the presence of 2-methylpropanal. *J. Mol. Catal.* **156**, 279–281 (2000).
10. Wang, A. & Jiang, H. Palladium-catalyzed direct oxidation of alkenes with molecular oxygen: general and practical methods for the preparation of 1,2-Diols, aldehydes, and ketones. *J. Org. Chem.* **75**, 2321–2326 (2010).
11. Khenkin, A. M. & Neumann, R. Aerobic oxidation of vicinal diols catalyzed by an Anderson-type polyoxometalate, $[IMo_6O_{24}]^{5-}$. *Adv. Synth. Catal.* **344**, 1017–1021 (2002).
12. Okamoto, T., Sasaki, K., Shimada, M. & Oka, S. Catalysis of aerobic C–C bond cleavage of 1,2-bis(4-methoxyphenyl)ethane-1,2-diol by meso-tetraphenylporphyri-natoiron(III). A model system for cytochrome $P\text{-}450_{scc}$-dependent glycol cleavage. *J. Chem. Soc. Chem. Commun.* **0**, 381–383 (1985).
13. Okamoto, T., Sasaki, K. & Oka, S. Biomimetic oxidation with molecular oxygen. Selective carbon-carbon bond cleavage of 1,2-diols by molecular oxygen and dihydropyridine in the presence of iron-porphyrin catalysts. *J. Am. Chem. Soc.* **110**, 1187–1196 (1988).
14. Amadio, E. et al. Efficient vanadium-catalyzed aerobic C–C bond oxidative cleavage of vicinal diols. *Adv. Synth. Catal.* **360**, 1–12 (2018).
15. Zhou, Z., Liu, M., Lv, L. & Li, C.-J. Silver(I)-catalyzed widely applicable aerobic 1,2-diol oxidative cleavage. *Angew. Chem. Int. Ed.* **57**, 2616–2620 (2018).
16. Obara, N., Hirasawa, S., Tamura, M., Nakagawa, Y. & Tomishige, K. Oxidative cleavage of vicinal diols with the combination of platinum and vanadium catalysts and molecular oxygen. *ChemCatChem* **8**, 1732–1738 (2016).
17. Felthouse, T. R., Fraundorf, P. B., Friedman, R. M. & Schosser, C. L. Expanded lattice ruthenium pyrochlore oxide catalysts I. Liquid-phase oxidations of vicinal diols, primary alcohols, and related substrates with molecular oxygen. *J. Catal.* **127**, 393–420 (1991).
18. Solmia, S. et al. The oxidative cleavage of *trans*-1,2-cyclohexanediol with O_2: catalysis by supported Au nanoparticles. *Appl. Catal. A* **557**, 89–98 (2018).
19. Escande, V., Lam, C. H., Coish, P. & Anastas, P. T. Heterogeneous sodium-manganese oxide catalyzed aerobic oxidative cleavage of 1,2-diols. *Angew. Chem. Int. Ed.* **56**, 9561–9565 (2017).
20. Escande, V., Lam, C. H., Grison, C. & Anastas, P. T. EcoMnOx, a biosourced catalyst for selective aerobic oxidative cleavage of activated 1,2-diols. *ACS Sustain. Chem. Eng.* **5**, 3214–3222 (2017).

21. Chen, B. et al. Metal-free and solvent-free oxidative coupling of amines to Imines with mesoporous carbon from macrocyclic compounds. *ACS Catal.* **5**, 2788–2794 (2015).
22. Chen, B., Shang, S. S., Wang, L. Y., Zhang, Y. & Gao, S. Mesoporous carbon derived from vitamin B12: a high-performance bifunctional catalyst for imine formation. *Chem. Commun.* **52**, 481–484 (2016).
23. Shang, S. S. et al. High catalytic activity of mesoporous Co–N/C catalysts for aerobic oxidative synthesis of nitriles. *Catal. Sci. Technol.* **6**, 5746–5753 (2016).
24. Shang, S. S., Dai, W., Wang, L. Y., Lv, Y. & Gao, S. Metal-free catalysis of nitrogen-doped nanocarbons for the ammoxidation of alcohols to nitriles. *Chem. Commun.* **53**, 1048–1051 (2017).
25. Chen, Y., Jie, S. S., Yang, C. Q. & Liu, Z. G. Active and efficient Co-N/C catalysts derived from cobalt porphyrin for selective oxidation of alkylaromatics. *Appl. Surf. Sci.* **419**, 98–106 (2017).
26. He, L., Weniger, F., Neumann, H. & Beller, M. Synthesis, characterization, and application of metal nanoparticles supported on nitrogen-doped carbon: catalysis beyond electrochemistry. *Angew. Chem. Int. Ed.* **55**, 12582–12594 (2016).
27. Zhou, P. et al. High performance of a cobalt-nitrogen complex for the reduction and reductive coupling of nitro compounds into amines and their derivatives. *Sci. Adv.* **3**, e1601945 (2017).
28. Wu, G., Chen, Z., Artyushkova, K., Garzon, F. H. & Zelenay, P. Polyaniline-derived non-precious catalyst for the polymer electrolyte fuel cell cathode. *Ecs Trans.* **16**, 159–170 (2008).
29. Xu, S. et al. Selective oxidation of 5-hydroxymethylfurfural to 2,5-furandicarboxylic acid using O_2 and a photocatalyst of co-thioporphyrazine bonded to g-C_3N_4. *J. Am. Chem. Soc.* **139**, 14775–14782 (2017).
30. Deng, J., Song, H. J., Cui, M. S., Du, Y. P. & Fu, Y. Aerobic oxidation of hydroxymethylfurfural and furfural by using heterogeneous Co_xO_y–N@C catalysts. *ChemSusChem* **7**, 3334–3340 (2014).
31. Zhong, W., Liu, H., Bai, C., Liao, S. & Li, Y. Base-free oxidation of alcohols to esters at room temperature and atmospheric conditions using nanoscale Co-based catalysts. *ACS Catal.* **5**, 1850–1856 (2015).
32. Nie, R. et al. A sandwich N-doped graphene/Co_3O_4 hybrid: an efficient catalyst for selective oxidation of olefins and alcohols. *Mater. Chem. A* **1**, 9037–9045 (2013).
33. Liu, W. G. et al. Single-atom dispersed Co–N–C catalyst: structure identification and performance for hydrogenative coupling of nitroarenes. *Chem. Sci.* **7**, 5758–5764 (2016).
34. Tang, C. H. et al. A Stable nanocobalt catalyst with highly dispersed CoN_x active sites for the selective dehydrogenation of formic acid. *Angew. Chem. Int. Ed.* **56**, 16616–16620 (2017).
35. Ma, R., He, L.-N., Liu, A.-H. & Song, Q.-W. Cu(II)-catalyzed esterification reaction via aerobic oxidative cleavage of C(CO)-C(alkyl) bonds. *Chem. Commun.* **52**, 2145–2148 (2016).
36. Kattel, S., Atanassov, P. & Kiefer, B. Catalytic activity of Co-N_x/C electrocatalysts for oxygen reduction reaction: a density functional theory study. *Phys. Chem. Chem. Phys.* **15**, 148–153 (2013).
37. Zhang, L. L. et al. Co–N–C Catalyst for C–C coupling reactions: On the catalytic performance and active sites. *ACS Catal.* **5**, 6563–6572 (2015).
38. Cui, X. J. et al. Synthesis and characterization of iron–nitrogen-doped graphene/core–shell catalysts: efficient oxidative dehydrogenation of N-heterocycles. *J. Am. Chem. Soc.* **137**, 10652–10658 (2015).
39. Lin, X. et al. Nitrogen-doped carbon nanotubes encapsulate cobalt nanoparticles as efficient catalysts for aerobic and solvent-free selective oxidation of hydrocarbons. *Green. Chem.* **19**, 2164–2173 (2017).
40. Zhao, L. et al. Covalent triazine framework catalytic oxidative cleavage of lignin models and organosolv lignin. *Green. Chem.* **20**, 1270–1279 (2018).
41. Schmidt, A. K. C. & Stark, C. B. W. The glycol cleavage in natural product synthesis: reagent classics and recent advances. *Synthesis* **46**, 3283–3308 (2014).

Acknowledgements

We gratefully acknowledge financial support from the National Natural Science Foundation of China (No. 21773227, 21403219, and 21773232), and Shandong Province Major Science and Technology Innovation Project (2108CXGC1102).

Author contributions

H.L. performed most of the experiments. L.W. helped with the completion of the scope with respect to diols substrates. L.W. wrote the manuscript with feedback from H.L. S.S. and Y.N. assisted with manuscript preparation, S.G. and L.W. designed and directed the projects. All authors contributed to the discussion.

Additional information

Supplementary information accompanies this paper at https://doi.org/10.1038/s42004-019-0116-5.

Competing interests: The authors declare no competing interests.

Reprints and permission information is available online at http://npg.nature.com/reprintsandpermissions/

Publisher's note: Springer Nature remains neutral with regard to jurisdictional claims in published maps and institutional affiliations.